

Search for lepton-flavour violating and lepton-number violating decays of the D^0 meson and observation of $D^0 \rightarrow K^- \pi^+ e^+ e^-$

Fergus WILSON*†

STFC Rutherford Appleton Laboratory, Harwell Campus, Didcot, Oxon, OX11 0QX, UK

E-mail: Fergus.Wilson@stfc.ac.uk

We report the observation of the rare charm decay $D^0 \rightarrow K^- \pi^+ e^+ e^-$ and a search for nine lepton-number-violating (LNV) and three lepton-flavor-violating (LFV) neutral charm decays of the type $D^0 \rightarrow h'^- h^- l'^+ l^+$ and $D^0 \rightarrow h'^- h^+ l'^\pm l^\mp$, where h and h' represent a K or π meson and l and l' an electron or muon. The analysis is based on 468 fb^{-1} of e^+e^- annihilation data collected at or close to the $\Upsilon(4S)$ resonance with the BaBar detector at the SLAC National Accelerator Laboratory. We find the $D^0 \rightarrow K^- \pi^+ e^+ e^-$ branching fraction in the invariant mass range $0.675 < m(e^+e^-) < 0.875 \text{ GeV}/c^2$ of the electron-positron pair to be $\mathcal{B}(D^0 \rightarrow K^- \pi^+ e^+ e^-) = (4.0 \pm 0.5 \pm 0.2 \pm 0.1) \times 10^{-6}$, where the first uncertainty is statistical, the second systematic, and the third due to the uncertainty in the branching fraction of the decay $D^0 \rightarrow K^- \pi^+ \pi^+ \pi^-$ used as a normalization mode. In a set of regions of $m(e^+e^-)$ where long-distance effects are potentially small, we determine a 90% confidence level (C.L.) upper limit on the branching fraction $\mathcal{B}(D^0 \rightarrow K^- \pi^+ \pi^+ \pi^-) < 3.1 \times 10^{-6}$. No significant signal is observed for any of the LFV and LNV modes, and we establish 90% C.L. upper limits on the branching fractions in the range $(1.0 - 30.6) \times 10^{-7}$. The limits are between one and three orders of magnitude more stringent than previous measurements.

XXIX International Symposium on Lepton Photon Interactions at High Energies - LeptonPhoton2019
August 5-10, 2019
Toronto, Canada

*Speaker.

†on behalf of the BABAR Collaboration

The decay $D^0 \rightarrow K^- \pi^+ e^+ e^-$ is expected to be very rare in the standard model (SM) as it cannot occur at tree level [1]. Short-distance contributions to the $D^0 \rightarrow K^- \pi^+ e^+ e^-$ branching fraction proceed through loop and box diagrams and are expected to be $\mathcal{O}(10^{-9})$ [2, 3]. Long-distance contributions could contribute at the level of $\mathcal{O}(10^{-6})$ through photon pole amplitudes or vector meson dominance [3]. Many models beyond the SM predict LFV or LNV, possibly at rates approaching those accessible with current data [4, 5]. LNV is a necessary condition for leptogenesis as an explanation of the baryon asymmetry of the Universe. If neutrinos are of Majorana type, the neutrino and antineutrino are the same particle and some LNV processes become possible [6].

We present the observation of the SM rare charm decay $D^0 \rightarrow K^- \pi^+ e^+ e^-$ and a search for nine $D^0 \rightarrow h'^- h^- \ell'^+ \ell^+$ LNV decays and three $D^0 \rightarrow h'^- h^+ \ell'^{\pm} \ell^{\mp}$ LFV decays, with data recorded with the *BABAR* detector at the PEP-II asymmetric-energy $e^+ e^-$ collider operated at the SLAC National Accelerator Laboratory. The data sample corresponds to 424 fb^{-1} of $e^+ e^-$ collisions collected at the center-of-mass (CM) energy of the $\Upsilon(4S)$ resonance (on peak) and an additional 44 fb^{-1} of data collected 40 MeV below the $\Upsilon(4S)$ resonance (off peak) [7]. The branching fractions for signal modes with zero, one, or two kaons in the final state are measured relative to the normalization decays $D^0 \rightarrow \pi^- \pi^+ \pi^+ \pi^-$, $D^0 \rightarrow K^- \pi^+ \pi^+ \pi^-$, and $D^0 \rightarrow K^- K^+ \pi^+ \pi^-$, respectively. The D^0 mesons are identified from the decay $D^{*+} \rightarrow D^0 \pi^+$ produced in $e^+ e^- \rightarrow c\bar{c}$ events. The *BABAR* detector is described in detail in Ref. [8].

Candidate D^0 mesons are formed from four charged tracks. Particle identification (PID) is applied to the charged tracks and the same criteria are applied to the signal and normalization modes. The four tracks must form a good-quality vertex with a χ^2 probability for the vertex fit greater than 0.005. A bremsstrahlung energy recovery algorithm is applied to the electrons, in which the energy of photon showers that are within a small angle (typically 35 mrad) of the initial electron direction are added to the energy of the electron candidate. The D^0 candidate momentum in the PEP-II center-of-mass system, p^* , must be greater than $2.4 \text{ GeV}/c$.

The candidate D^{*+} is formed by combining the D^0 candidate with a charged pion with a momentum in the laboratory frame greater than $0.1 \text{ GeV}/c$. A vertex fit is performed with the D^0 mass constrained to its known value and the requirement that the D^0 meson and the pion originate from the interaction region. The χ^2 probability of the fit is required to be greater than 0.005.

For $D^0 \rightarrow K^- \pi^+ e^+ e^-$ and the normalization modes, the signal and normalization yields are extracted with a two-dimensional unbinned maximum-likelihood (ML) fit to the D^0 meson mass $m(D^0)$ and the mass difference, $\Delta m = m(D^{*+}) - m(D^0)$, between the reconstructed masses of the D^{*+} and D^0 candidates; the ranges are $1.81 < m(D^0) < 1.91 \text{ GeV}/c^2$ and $0.143 < \Delta m < 0.148 \text{ GeV}/c^2$. The normalization modes Δm and $m(D^0)$ distributions are each represented by multiple Cruiff [9] or Crystal Ball [10] functions. For the $D^0 \rightarrow K^- \pi^+ e^+ e^-$ signal, a Gaussian-like function with different lower and upper widths is used for both Δm and $m(D^0)$. The backgrounds are represented by an ARGUS threshold function [11] for Δm and a Chebyshev polynomial for $m(D^0)$. All parameters, apart from the ARGUS threshold endpoint, are allowed to vary.

For the LFV and LNV signal decays, the selection process is modified. A multivariate discriminant (MVA) using nine observables as input is applied to the signal modes to reduce the backgrounds from $e^+ e^- \rightarrow c\bar{c}$. The observables are based on the kinematics of the final-state particles and the event shape. The D^0 meson mass $m(D^0)$ is required to be within three times the reconstructed $m(D^0)$ mass resolution, with the resolution depending on the number of e^{\pm} in

the decay. The signal yields are extracted with a one-dimensional unbinned ML fit to the range $0.141 < \Delta m < 0.201 \text{ GeV}/c^2$ for signal modes with two kaons and $0.141 < \Delta m < 0.149 \text{ GeV}/c^2$ for all other signal modes. The signal probability density function (PDF) is a Cruijff function with parameters obtained by fitting the signal MC. The background is modeled with an ARGUS function with an endpoint that is set to the same value that is used for the normalization modes. The signal PDF parameters and the ARGUS endpoint parameter are fixed in the fit. All other background parameters and the signal and background yields are allowed to vary.

The main sources of systematic uncertainty in the branching fraction determinations are associated with the model parameterizations used in the fits and the normalization procedure, signal MC modeling, MVA optimisation, fit bias, tracking and PID efficiencies, luminosity, backgrounds from intermediate decays to $e^+ e^- \gamma$, and the normalization mode branching fraction. Some of the tracking and PID systematic effects cancel in the branching fraction determinations since they affect both the signal and normalization modes. The model parameterizations and the MVA optimisation are the largest contributors to the systematic uncertainties.

The fitted yields for the normalization modes $D^0 \rightarrow \pi^- \pi^+ \pi^+ \pi^-$, $D^0 \rightarrow K^- \pi^+ \pi^+ \pi^-$, and $D^0 \rightarrow K^- K^+ \pi^+ \pi^-$ are 28470 ± 220 , 260870 ± 520 , and 8480 ± 110 , with reconstruction efficiencies $(24.7 \pm 0.2)\%$, $(20.1 \pm 0.2)\%$, and $(19.2 \pm 0.2)\%$, respectively.

For the $D^0 \rightarrow K^- \pi^+ e^+ e^-$ signal mode, the fitted yield is 68 ± 9 candidates in the range $0.675 < m(e^+ e^-) < 0.875 \text{ GeV}/c^2$. The significance S of the signal yield in this mass range, is 9.7 standard deviations (σ). The branching fraction $\mathcal{B}(D^0 \rightarrow K^- \pi^+ e^+ e^-)$ in the mass range $0.675 < m(e^+ e^-) < 0.875 \text{ GeV}/c^2$ is determined to be $(4.0 \pm 0.5 \pm 0.2 \pm 0.1) \times 10^{-6}$, where the first uncertainty is statistical, the second systematic, and the third comes from the uncertainty in $\mathcal{B}(D^0 \rightarrow K^- \pi^+ \pi^+ \pi^-)$ [15]. The fits are shown in Fig. 1, together with the background-subtracted projections onto $m(e^+ e^-)$ and $m(K^- \pi^+)$. The branching fraction and the distributions are similar to those seen in Ref. [12] for the decay $D^0 \rightarrow K^- \pi^+ \mu^+ \mu^-$.

The fitted signal yield in the region of the ϕ meson, defined as the mass range $1.005 < m(e^+ e^-) < 1.035 \text{ GeV}/c^2$, is $3.8_{-1.9}^{+2.7}$; the statistical significance S is 1.8σ . The branching fraction is determined to be $(2.2_{-1.1}^{+1.5} \pm 0.6) \times 10^{-7}$ and the 90% branching fraction upper limit is 0.5×10^{-6} ,

We repeat the fit to Δm and $m(D^0)$ in the ‘‘continuum’’ $m(e^+ e^-)$ region that is predicted to be relatively unaffected by intermediates states, and is defined by excluding the following $m(e^+ e^-)$ mass ranges: $m(e^+ e^-) < 0.2 \text{ GeV}/c^2$, $0.675 < m(e^+ e^-) < 0.875 \text{ GeV}/c^2$, $0.491 < m(e^+ e^-) < 0.560 \text{ GeV}/c^2$, $0.902 < m(e^+ e^-) < 0.964 \text{ GeV}/c^2$, and $1.005 < m(e^+ e^-) < 1.035 \text{ GeV}/c^2$. These correspond to ranges dominated by the decays of the π^0 and ρ^0/ω mesons or potentially affected by the decays of η , η' , and ϕ mesons, respectively. These $m(e^+ e^-)$ mass ranges exclude 90% of any remaining simulated candidates that pass the selection criteria. The number of background decays from intermediate states in the continuum region is predicted to be 9.9 ± 0.9 , dominated by the decay $\rho^0/\omega \rightarrow e^+ e^-$ with $m(e^+ e^-)$ less than $0.675 \text{ GeV}/c^2$. The fitted yield in the continuum region, after the subtraction of this background, is 19 ± 7 , with a statistical significance $S = 2.6\sigma$. This corresponds to $(1.6 \pm 0.6 \pm 0.7) \times 10^{-6}$. The result is not significant and we determine a 90% confidence level (C.L.) branching fraction upper limit of 3.1×10^{-6} using the frequentist approach of Feldman and Cousins [13]. The $m(e^+ e^-)$ distribution is shown in Fig. 2.

For the LFV and LNV modes, no significant signal is seen and 90% C.L. branching fraction upper limits between $(1.0 - 30.6) \times 10^{-7}$ are determined. These are between one and three orders

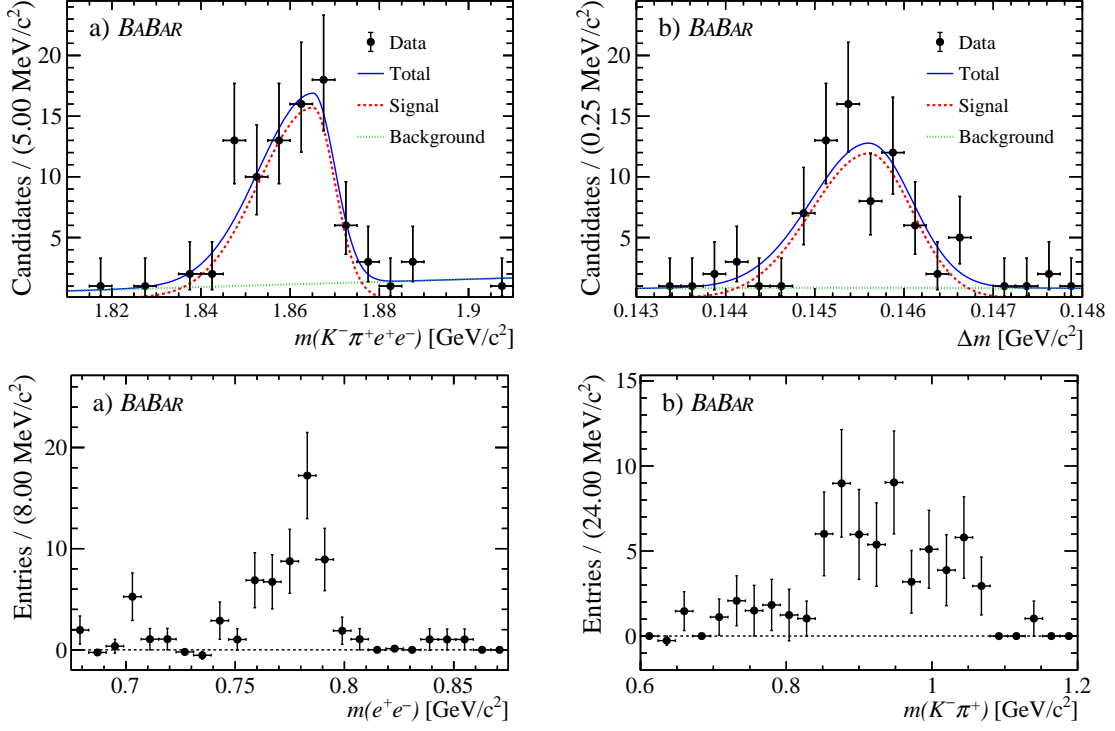


Figure 1: Fits to $D^0 \rightarrow K^- \pi^+ e^+ e^-$ data sample for (top left) D^0 mass and (top right) Δm in the restricted phase space $0.675 < m(e^+ e^-) < 0.875 \text{ GeV}/c^2$. Also shown is the projection of the background-subtracted fitted signal as a function of (bottom left) $m(e^+ e^-)$ and (bottom right) $m(K^- \pi^+)$.

of magnitude more stringent than previous results. The fits are shown in Fig. 3 and the results are given in Table 1.

Table 1: Summary of fitted signal yields with statistical and systematic uncertainties, reconstruction efficiencies, branching fractions with statistical and systematic uncertainties, 90% C.L. branching fraction upper limits (U.L.), and the previous limits [15, 16].

Decay mode	N_{sig} (candidates)	ϵ_{sig} (%)	\mathcal{B} ($\times 10^{-7}$)	$\mathcal{B}_{90\%}^{\text{U.L.}}$ ($\times 10^{-7}$)	$\mathcal{B}_{90\%}^{\text{U.L.}}$ [PDG] ($\times 10^{-7}$)
$\pi^- \pi^- e^+ e^+$	$0.22 \pm 3.15 \pm 0.54$	4.38	$0.27 \pm 3.90 \pm 0.67$	9.1	1120
$\pi^- \pi^- \mu^+ \mu^+$	$6.69 \pm 4.88 \pm 0.80$	4.91	$7.40 \pm 5.40 \pm 0.91$	15.2	290
$\pi^- \pi^- e^+ \mu^+$	$12.42 \pm 5.30 \pm 1.45$	4.38	$15.41 \pm 6.59 \pm 1.85$	30.6	790
$\pi^- \pi^+ e^\pm \mu^\mp$	$1.37 \pm 6.15 \pm 1.28$	4.79	$1.55 \pm 6.97 \pm 1.45$	17.1	150
$K^- \pi^- e^+ e^+$	$-0.23 \pm 0.97 \pm 1.28$	3.19	$-0.38 \pm 1.60 \pm 2.11$	5.0	28 [16]
$K^- \pi^- \mu^+ \mu^+$	$-0.03 \pm 2.10 \pm 0.40$	3.30	$-0.05 \pm 3.34 \pm 0.64$	5.3	3900
$K^- \pi^- e^+ \mu^+$	$3.87 \pm 3.96 \pm 2.36$	3.48	$5.84 \pm 5.97 \pm 3.56$	21.0	2180
$K^- \pi^+ e^\pm \mu^\mp$	$2.52 \pm 4.60 \pm 1.35$	3.65	$3.62 \pm 6.61 \pm 1.95$	19.0	5530
$K^- K^- e^+ e^+$	$0.30 \pm 1.08 \pm 0.41$	3.25	$0.43 \pm 1.54 \pm 0.58$	3.4	1520
$K^- K^- \mu^+ \mu^+$	$-1.09 \pm 1.29 \pm 0.42$	6.21	$-0.81 \pm 0.96 \pm 0.32$	1.0	940
$K^- K^- e^+ \mu^+$	$1.93 \pm 1.92 \pm 0.83$	4.63	$1.93 \pm 1.93 \pm 0.84$	5.8	570
$K^- K^+ e^\pm \mu^\mp$	$4.09 \pm 3.00 \pm 1.59$	4.83	$3.93 \pm 2.89 \pm 1.45$	10.0	1800

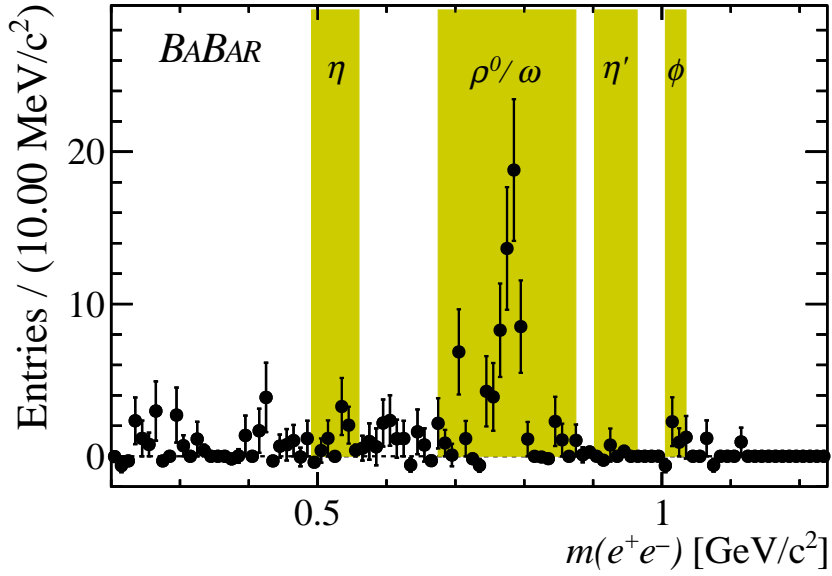
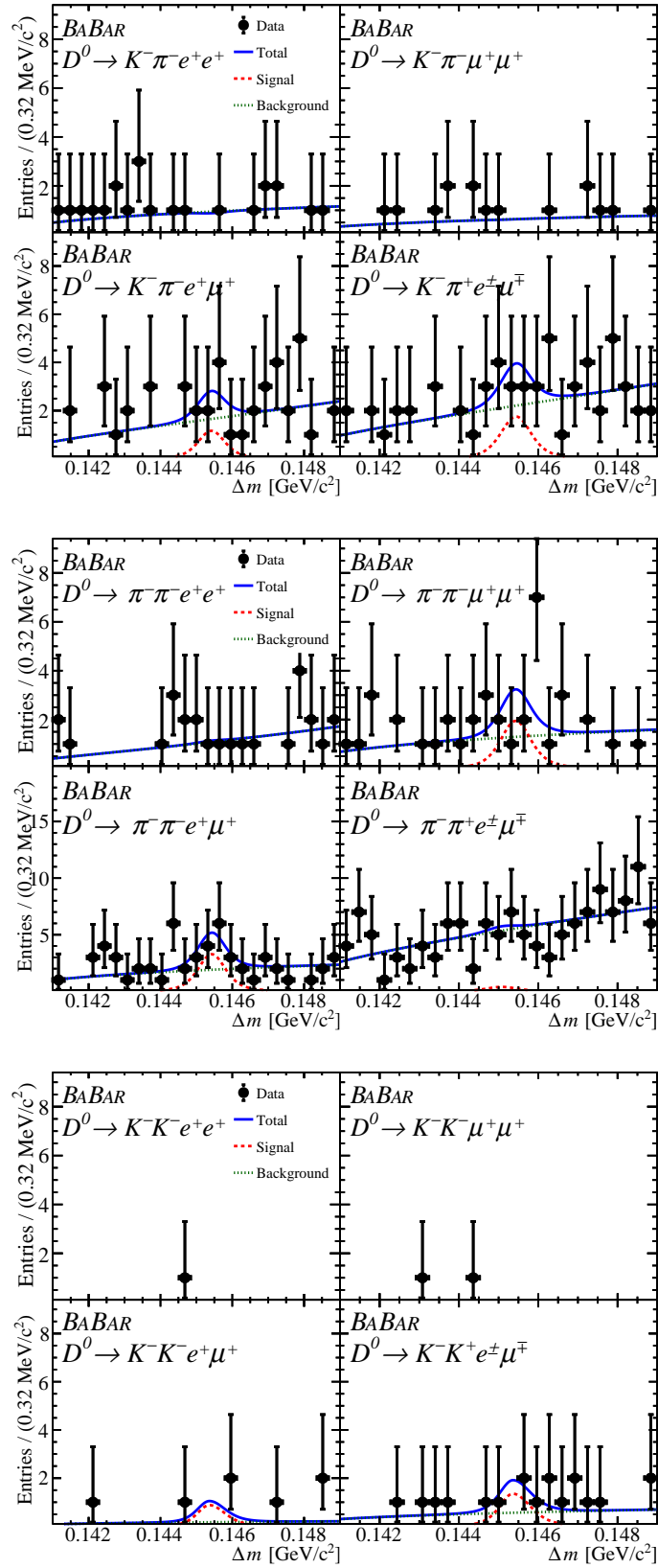


Figure 2: Projection of the fits to the $D^0 \rightarrow K^- \pi^+ e^+ e^-$ data distributions onto $m(e^+ e^-)$ for candidates with $m(e^+ e^-) > 0.2 \text{ GeV}/c^2$. The background has been subtracted using the *sPlot* technique [14]. The shaded yellow regions are excluded from the continuum region.

References

- [1] S.L. Glashow, J. Iliopoulos and L. Maiani, Phys. Rev. D **2**, 1285 (1970).
- [2] A. Paul, I.I. Bigi and S. Recksiegel, Phys. Rev. D **83**, 114006 (2011).
- [3] A.J. Schwartz, Mod. Phys. Lett. **A8**, 967 (1993).
- [4] S. de Boer and G. Hiller, Phys. Rev. D **93**, 074001 (2016).
- [5] S. Fajfer and N. Košnik, Eur. Phys. Jour. C **75**, 567 (2015).
- [6] E. Majorana, Nuo. Cim. **14**, 171 (1937).
- [7] J.P. Lees *et al.*, (BABAR Collaboration), Nucl. Instrum. Methods Phys. Res., Sect. A **726**, 203 (2013).
- [8] B. Aubert *et al.*, (BABAR Collaboration), Nucl. Instrum. Methods Phys. Res., Sect. A **479**, 1 (2002); A **729** 615 (2013).
- [9] The Cuijff function is a centered Gaussian with different left-right resolutions and non-Gaussian tails: $f(x) = \exp(-(x-m)^2 / (2\sigma_{L,R}^2 + \alpha_{L,R}(x-m)^2))$.
- [10] T. Skwarnicki, Thesis, Institute of Nuclear Physics, Krakow, DESY-F31-86-02.
- [11] H. Albrecht *et al.*, (ARGUS Collaboration), Phys. Lett. B **241**, 278 (1990).
- [12] R. Aaij *et al.*, (LHCb Collaboration), Phys. Lett. B **757**, 558 (2016).
- [13] G. Feldman and R.D. Cousins, Phys. Rev. D **57**, 3873 (1998).
- [14] M. Pivk and F.R. le Diberder, Nucl. Instrum. Methods Phys. Res., Sect. A **555**, 356 (2005).
- [15] Particle Data Group, M. Tanabashi *et al.*, Phys. Rev. D **98**, 032001 (2018).
- [16] M. Abkilim *et al.*, (BES-III Collaboration), Phys. Rev. D **99**, 112002 (2019).


 Figure 3: Fits to nine $D^0 \rightarrow h'^- h^- \ell'^+ \ell^+$ LNV decays and three $D^0 \rightarrow h'^- h^+ \ell'^{\pm} \ell^{\mp}$ LFV decays.